Stony Brook University

Stony Brook University

Characterization of Trifunctional Glycinamide Ribonucleotide Synthetase and its Role in Purinosome Complex

A Thesis Presented

by

Iva Chitrakar

to

The Graduate School

in Partial Fulfillment of the

Requirements

for the Degree of

Master of Science

in

Biochemistry and Cell Biology

Stony Brook University

December 2014

Stony Brook University

The Graduate School

Iva Chitrakar

We, the thesis committee for the above candidate for the

Master of Science degree, hereby recommend

acceptance of this thesis.

Jarrod French
Assistant Professor- Department of Biochemistry and Cell Biology

Martin Kaczocha
Department of Anesthesiology

This thesis is accepted by the Graduate School

Charles Taber
Dean of the Graduate School

Abstract of the Thesis

Characterization of Trifunctional Glycinamide Ribonucleotide Synthetase and its Role in Purinosome Complex

by

Iva Chitrakar

Master of Science

in

Biochemistry and Cell Biology

Stony Brook University

December 2014

The human *de novo* purine biosynthetic pathway consists of six proteins, which come together to form a protein complex called the purinosome. The tri-functional enzyme, TGART, which contains three domains, is one of the purinosome proteins. Protein-protein interaction studies have shown that TGART, along with two other *de novo* purine pathway proteins FGAMS and PPAT, is at the core of purinosome complex. Little is known, however about the interacting surface, stoichiometry or interaction mechanism. In order to understand this, we hope to solve the X-ray crystal structure of full-length human TGART, run quantitative protein interaction measurements on TGART, FGAMS and PPAT and decipher the molecular organization of these proteins. To date all three individual domains as well as a fusion domain with last two of the three domains of TGART have been expressed and purified to homogeneity.

Table of Contents

List of Figures

List of Abbreviations

AICAIRT	aminoimidazolecarboxamide ribonucleotide transformylase
AIRS	animoimidazole ribonucleotide synthetase
AMP	adenosine monophosphate
ASL	adenylsuccinate lyase
AMP-PNP	adenylyl iminodiphosphate
CAIRS	carboxyaminoimidazole ribonucleotide synthase
CD	circular dichroism
DLS	dynamic light scattering
FGAM	formylglycinamide ribonucleotide synthetase
GARS	glycinamide ribonucleotide synthetase
GART	glycinamide ribonucleotide formyltransferase
HPRT	hypoxanthine phosphoribosyl transferase
IMP	inosine monophosphate
IMPCH	inosine monophosphate cyclohydrolase
P*i*	inorganic phosphate
PPAT	phosphoribosylpyrophosphate amidotransferase
PPI	protein- protein interaction
PRA	phosphorinosyl amine
PRPP	phosphoribosylpyrophosphate
SAICAR	succinoaminoimidazolecarboxamide ribonucleotide synthetase

SAXS small angle X-ray scattering

SEC size exclusion chromotography

SPR surface plasmon resonance

TGART trifunctional-GART

- Fl-*Hs*TGART full length- *Homo sapien* TGART

Acknowledgments

I would like to thank Dr. French for letting me be a member of his lab and for his guidance. I would also like to thank Dr. Kaczocha for agreeing to be my second reader especially because my request was out of the blue and my lab members Ben, Cindy, Roger and Sally for tolerating my music.

1. Introduction

1.1 Purines and their significance

Purines are nitrogenous bases composed of a pyrimidine and an imidazole ring. Adenine and guanine are purines and along with pyrimidines (thymine, cytosine and uracil) they are the building blocks for DNA and RNA. Purines are also integral biomolecules for energy storage in the form of ATP/ GTP, for cell signaling as cAMP/cGMP and as co-factors for many enzymes (1, 2). Genetic defects of purine metabolism can cause diseases such as immunodeficiency, mental retardation, and seizures (3, 4). Two unique pathways, the salvage pathway and the *de novo* pathway, work together to control intracellular purine levels (1). However, deficiency or acceleration of these pathways results in diseases. For instance, deficiency in salvage pathway activity leads to increased activity of the *de novo* pathway, contributing to high level of uric acid, which leads to inflammatory arthritis (5). Disorders like malignant cell growth and proliferation are one of the consequences of increased activity of *de novo* pathway (4). This makes the purine biosynthetic pathway a common drug target. Purine or pyrimidines antimetabolites are 20% of approved oncology drugs and other therapeutic drugs that disrupt purine metabolic enzymes that require folate cofactors (1, 4, 6) are used for treating autoimmune disorders like rheumatoid arthritis.

1.2 Two pathways involved in purine synthesis

A basal purine level in cells is essential and maintained *via* two complementary pathways, the salvage pathway and the *de novo* biosynthetic pathway. The salvage pathway [Fig. 1A] is a low energy mechanism to maintain the purine level under normal cellular conditions. It uses preformed bases accumulated due to degradation of RNA and DNA to generate purine

nucleotides. A single enzyme, hypoxanthine phosphoribosyl transferase (HPRT), catalyzes the reaction of cellular hypoxanthine and phosphoribosylpyrophosphate (PRPP) to make inosine monophosphate (IMP) (7, 8).

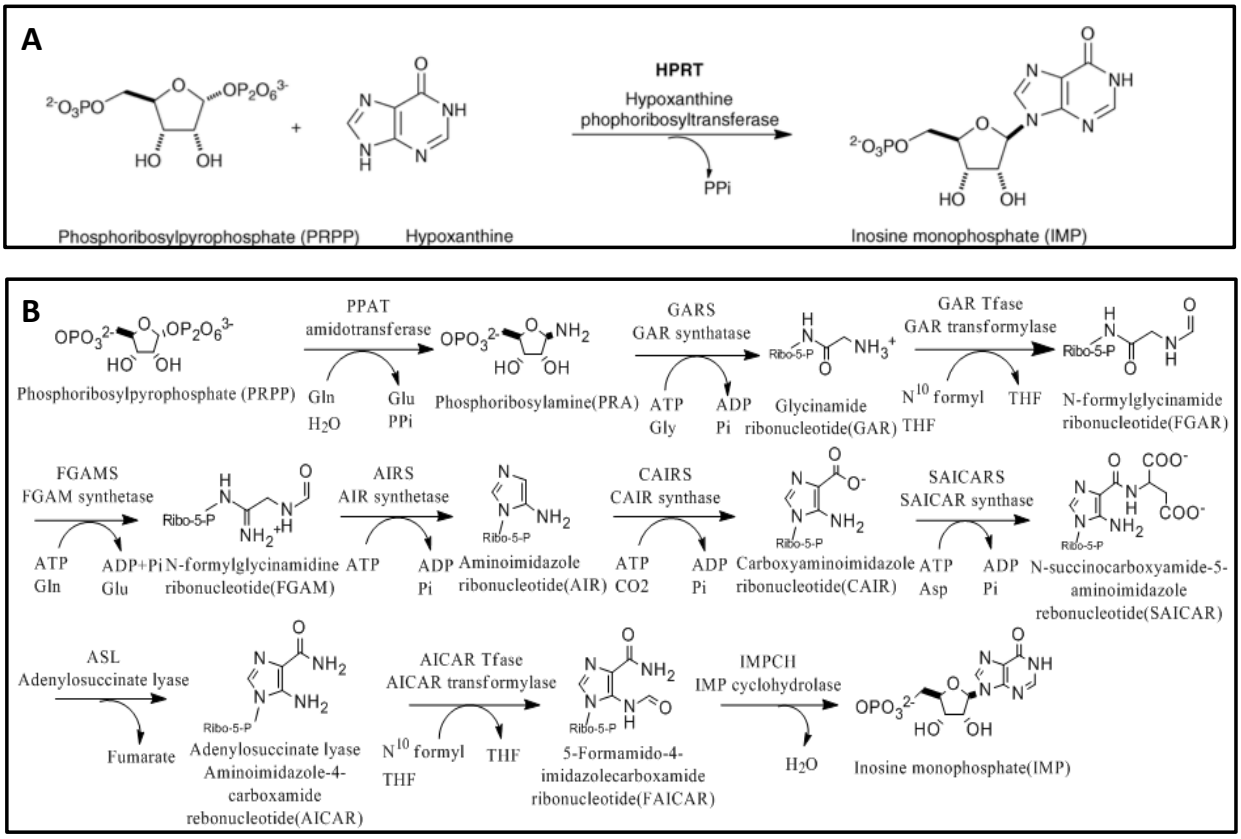

Figure 1 Cellular pathways involved in purine synthesis: A) The salvage pathway involves HRPT that uses PRPP and hypoxanthine to make IMP. **B)** The *de novo* purine biosynthesis has 10 conserved enzymatic steps that processes PRPP to make IMP. The monofunctional enzymes **PPAT, FGAMS** and **ASL** catalyze steps 1, 4 and 8 respectively. The bifunctional enzymes **ATIC** and **PAICS** catalyze steps 6,7 and 9,10 respectively. Trifunctional **GART** catalyzes steps 2, 3 and 5. Both the pathways produce IMP that is used by two distinct pathways to make adenine and guanine. Zhao *et al.* 2013

The *de novo* biosynthesis pathway [Fig 1B] is an energy intensive, highly regulated and conserved ten steps enzymatic process. It increases the size of purine pool required during events such as cell division (7). While bacteria use ten to twelve enzymes to complete the conversion of PRPP to IMP, humans use only six gene products. These include three monofunctional enzymes phosphoribosylpyrophosphate amidotransferase (PPAT), formylglycinamide ribonucleotide

synthetase (FGAMS) and adenylsuccinate lyase (ASL), two bifunctional enzymes ATIC composed of aminoimidazolecarboxamide ribonucleotide transformylase (AICART) and inosine monophosphate cyclohydrolase (IMPCH) and PAICS composed of carboxyaminoimidazole ribonucleotide synthase (CAIRS) and succinoaminoimidazolecarboxamide ribonucleotide synthetase (SAICARS), and a trifunctional enzyme TGART composed of glycinamide ribonucleotide synthetase (GARS), GAR transferase (GART) and animoimidazole ribonucleotide synthetase (AIRS). The final product from both the *de novo* and salvage pathways feed two different downstream pathways to make ATP and GTP [Fig 2](7, 9, 10).

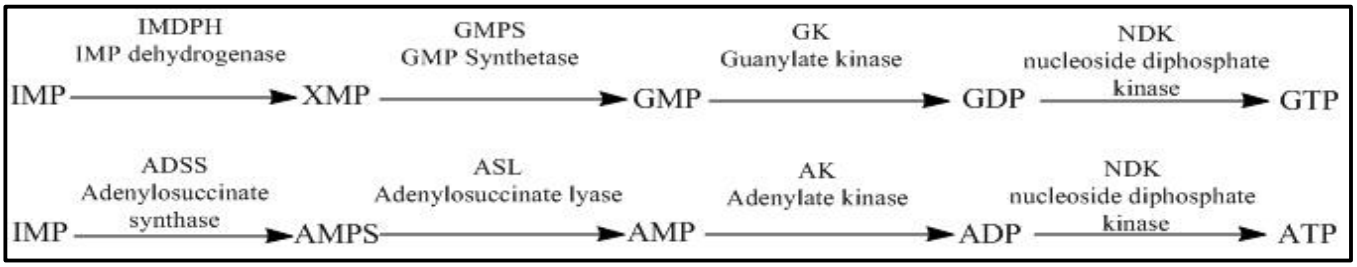

Figure 2 Pathway post-IMP synthesis: IMP produced by the salvage pathway and the *de novo* pathway is used by two distinct pathways to make GTP and ATP. Note: ASL which catalyzes step 8 of *de novo* pathway is involved in ATP synthesis. Zhao *et al.* 2013

1.3 Purinosome complex in *de novo* purine biosynthesis

Qualitative studies of the *de novo* pathway proteins have indicated they form a functional protein complex (7, 11, 12). The protein complex formation, called the purinosome, is supported by co-purification of proteins (1), presence of unstable intermediates, kinetics undermining free diffusion models (13, 14), and protein-protein interaction data (PPI) (15). Fluorescent studies have confirmed purinosome formation during *de novo* purine biosynthesis (16). An *et al.* showed cytoplasmic coclustering of endogenous and transiently transfected human TGART and human FGAMS in purine-deprived media [Fig. 3]. Their study also revealed reversibility of purinosome protein complex formation as demonstrated by colocalization of these proteins in the cytoplasm

in purine-deprived media followed by complex dissociation (16) when introduced to purine-rich media showing the pathway is impacted by its cellular milieu.

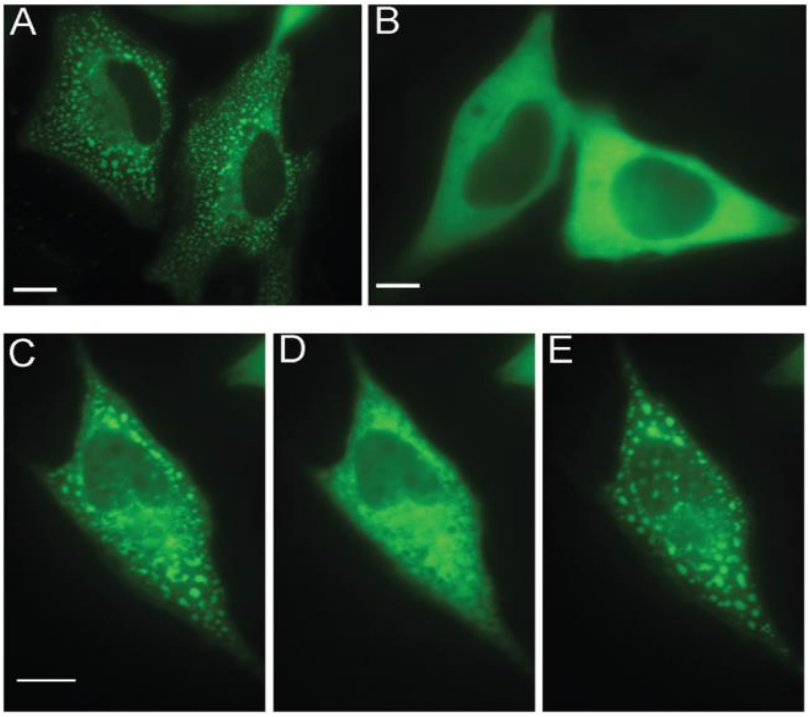

Figure 3: Colocalization of *de novo* purine biosynthetic proteins: A) shows a HeLa cell showing clustering of FGAMS-GFP into purinosomes under conditions of purine depletion, while B) shows the diffuse distribution of the FGAMS-GFP under 'purine-rich' conditions. C) through E) show that the phenomenon is reversible when you go from purine depletion (C) to purine rich (D) and then back to purine depletion (E).

1.4 Factors known to affect purinosome complex formation

Cellular conditions have a strong impact on purinosome complex formation or dissociation as affirmed by the proteins' behavior in purine-deprived and purine-rich conditions. The complex formation is assisted by a number of cellular mechanisms. Along with colocalization of *de novo* purine biosynthetic proteins, Hsp70/ Hsp 90 and a number of co-chaperones have been shown to colocalize with the purinosome complex. Inhibition and knockdown experiments of Hsp70/90 and co-chaperones were shown to suppress purinosome

complex formation signifying the Hsp's role in formation or stabilization (17). Similarly, fluorescent live cell imaging recognized colocalization of microtubules and purinosome complex, which was deterred in the absence of microtubules(18). Furthermore, casein kinase II (CK2) activity was shown to stimulate the complex formation while inhibition of CK2 prompted complex dissociation (19). This dependency of purinosome on other cellular pathways shows that the pathway is dynamic and highly regulated.

1.5 Kinetics and role of TGART in purine synthesis

TGART catalyzes steps two, three and five in the 10-step *de novo* biosynthetic pathway in *E.coli* and mammals (1, 7, 10). While it is a product of individual mono-functional genes in *E. coli,* it is a product of a single gene, located on chromosome 21 in humans, resulting in a trifunctional enzyme (7). The TGART polypeptide consists of three domains, each catalyzing a separate reaction in the pathway. The N-terminal domain is a GAR synthetase (GARS), the C-terminus has GAR transformylase (GART) activity, while the central domain is an aminoimidazole ribonucleotide synthetase (AIRS) (2, 5, 9). Linker regions that are believed to be composed of relatively disordered loops join these domains (20).Because this enzyme catalyzes multiple non-sequential steps in purine biosynthesis, one leading hypothesis is that it physically interacts with FGAMS to provide some functional advantage.

A number of variations of TGART gene arrangements are found in eukaryotes(7). The enzymes in purine biosynthetic pathways are labeled with prefix Pur in microorganisms and GARS, GART and AIRS are also known as PurD, PurN and PurM, respectively. A bifunctional enzyme, PurD and PurM, is present in yeast. PurD-PurM dimers are found in reptiles and a PurM-PurM' monomer can be found in drosophila [Fig 4] (7). Despite gene arrangement

variations in different organisms, studies have established conserved enzyme kinetics and functions (7-9).

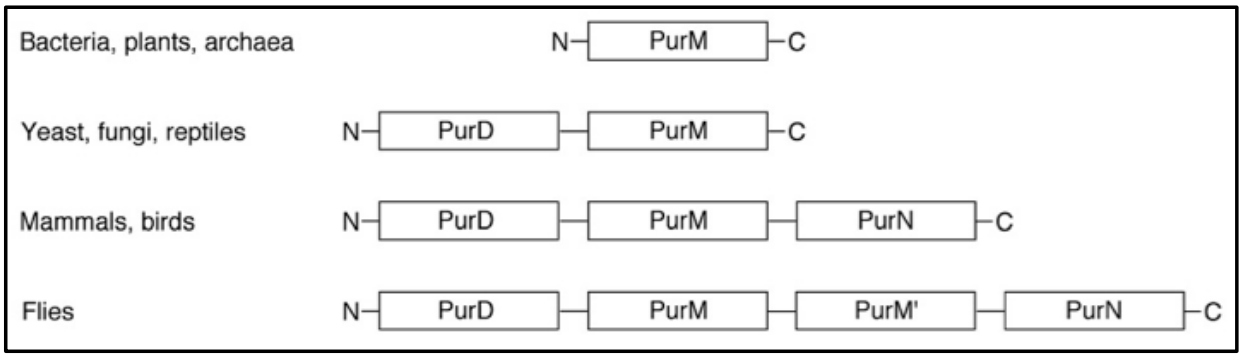

Figure 4 Variation in gene organization TGART: In *E. coli* and relative microorganisms, GARS, AIRS and GART are commonly identified as PurD, PurM and PurN, respectively. Zhang *et al.* 2008

GARS, GART and AIRS catalyze step 2, 3 and 5 of the purine *de novo* biosynthetic pathway, respectively [Fig. 5](10). GARS is an ATP-grasp enzyme that ligates glycine to phosphoribosylamine (PRA) in an ATP-dependent fashion, producing GAR, ADP and P_i (2, 9, 21, 22). GART transfers a formyl group from its cofactor 10-formyltetrahydrofolate to GAR to form FGAR in an ATP-dependent reaction (9, 23, 24). AIRS uses the amide in FGAM to catalyze FGAM's ring closure to make AIR and P_i.

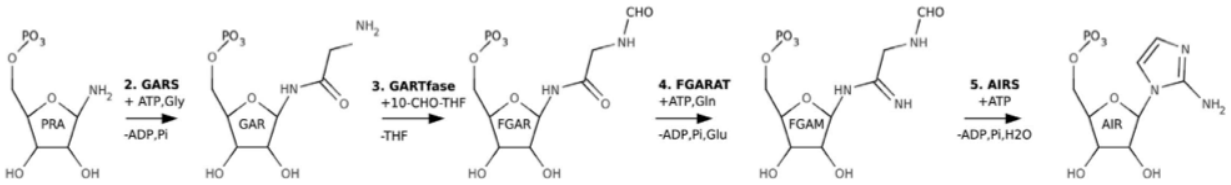

Figure 5 Steps 2-5 of the *de novo* pathway: GARS uses PPAT product PRA to form GAR which is GART's substrate. GART produces FGAR processed by FGAMS to form FGAM that will be processed by AIRS. Li *et al.* 1999

1.6 Known structure of GARS, GART and AIRS in prokaryotes and eukaryotes

X-ray crystal structures show GARS is a monomer with three domains [Fig. 6]. The 48kDa protein has A and C domains that form a core PRA binding site with an extended flexible

B domain covering the active site (9, 14, 25). The C-terminus (C domain) is composed of six α-helices around an eight-stranded anti-parallel β-sheets divided into 2 subdomains, C1 and C2, the former consisting of five β-strands and four α-helices and the latter with the last three β-strands and two α-alpha helices(20). The N-terminus (A domain) of GARS is composed of two α-helices that skirt a five stranded β-sheets, and the central B domain is four anti-parallel β strands and a disordered loop that transforms into an ordered state in the presence of ATP. Together, the A and B domain form the ATP binding site, with a glycine positioned by the ATP -phosphate (26).

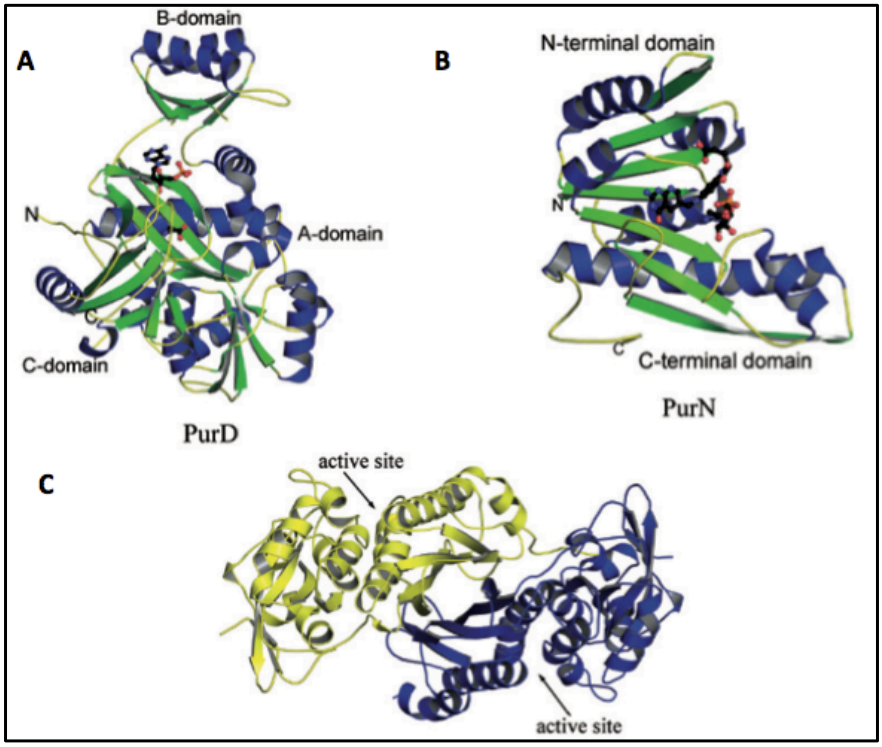

Figure 6 X-ray crystal structures of TGART domains: A) *Geobacillus kaustophilus* GARS (PurD) has an ATP-grasp domain with domains A and C for substrate core while domains A and B form the ATP binding site. Glycine and AMP are in the active site in ball-and-stick representation **B)** *E. coli* GART (PurN) also an ATP-grasp enzyme has similar structure and active site to PurD. Substrate glyciamide ribonucleotide and inhibitor 5-deaza-5,6,7,8-tetrahydrafolate are in ball-and-stick representation. **C)** *E. coli* AIRS (PurM) belong to PurM superfamily. Here it is shown in its dimer configuration with four-stranded β-sheets as the dimer interface. Zhang *et al.* 2008

GART or PurN, which catalyzes the third step in *de novo* purine biosynthesis, is a 25 kDa protein divided into two domains in both *E. coli* and mammals (23, 27). The N-terminal

domain has four α-helices followed by four β-strands and the C-terminal domain has two α-helices and two β-strands, such that the core is β-strands surrounded by α-helices [Fig. 6] (20). Two loops from the C-terminal domain and a single loop from the N-terminal domain form a 10-formylTHF binding site. *E.coli* and related microorganisms have GART homodimeric PurT (20), an ATP-grasp enzyme that shares similarity with GARS (26). The A and B domains of PurT form an ATP binding site while the A and C domains form a GAR binding site.

The third component of human TGART (*Hs*TGART), AIRS is classified into a distinct PurM superfamily of ATP- binding enzyme (28, 29). The 37 kDa PurM protein has an N-terminal domain of four-stranded β-sheets skirted by four α-helices and a C-terminus with six-stranded β-sheets with seven α-helices [Fig. 6] (20). In yeast, AIRS is a homodimer with N-terminal β-strands as the dimer interface while drosophila has a pseudodimer because of its PurM-PurM' arrangement (7). This has led to inference that full-length human TGART (fl-*Hs*TGART) exists as a dimer with PurM as the interacting surface; this was also confirmed by small angle X-ray scattering (SAXS) experiments (20).

1.7 Structural organization of TGART and interaction with other purinosome proteins

While structures of mono-functional gene TGART enzymes in *E. coli* and relevant microorganisms and individual domains of mammalian TGART have been characterized (9, 20, 25, 27, 28), the full length TGART or fusions of GARS-AIRS or AIRS-GART have not been determined yet. Attempts to crystallize full-length TGART have not been successful, likely due to the disordered nature of the polypeptide, and its susceptibility to proteolysis (20). Using, SAXS however Welin *et al.*shed some light on the organization of fl-*Hs*TGART in solution, indicating a dimer conformation with AIRS maintaining the dimeric configuration [Fig. 7]. The

other two domains were observed to be relatively disordered and the full-length enzyme was observed in an extended conformation.

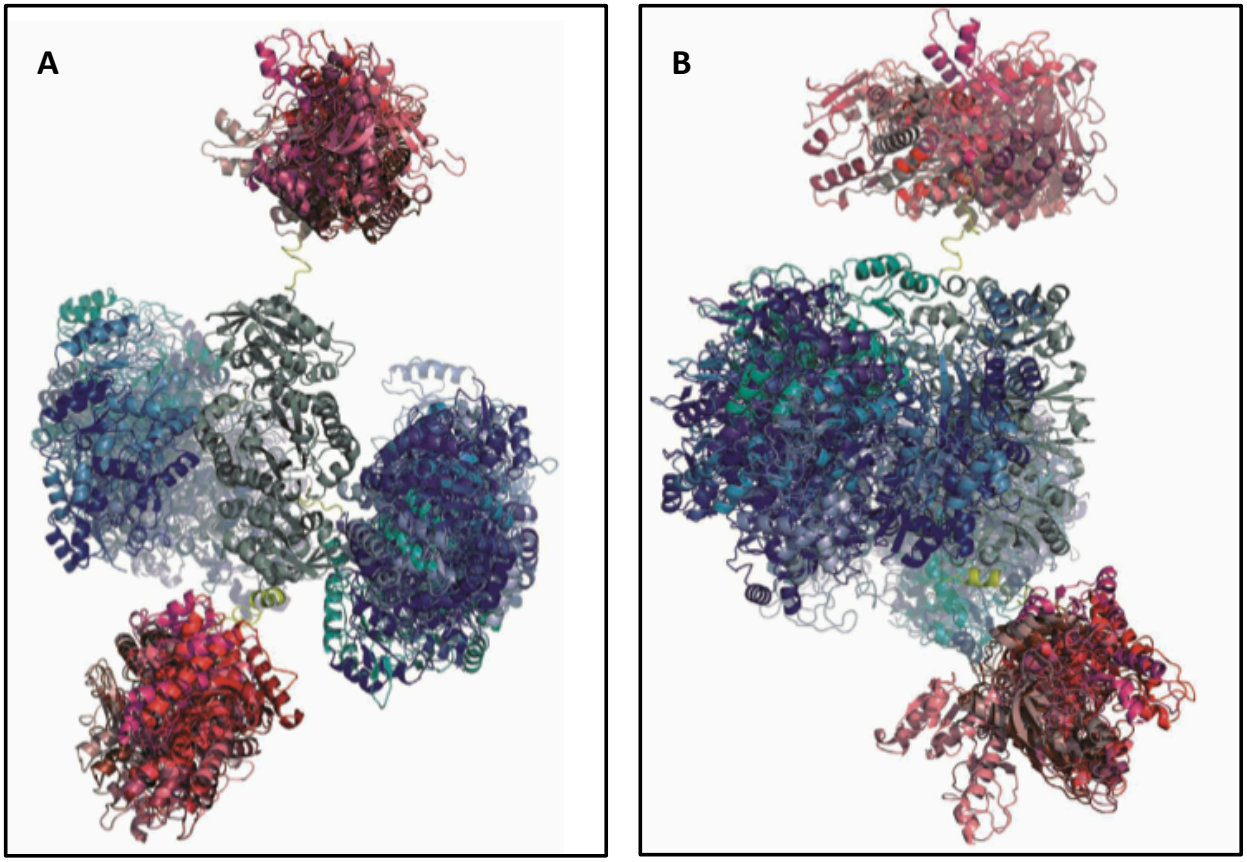

Figure 7 Full length *Hs*TGART configuration inferred from solution small angle X-ray scattering (SAXS): The conformational configuration is generated from ten rigid-body superimposed around AIRS' structure (shades of gray) with relatively flexible GARS (shades of blue) and GART (shades of red) connected by linkers (yellow). **A)** View along the dimer axis AIRS **B)** Orientation rotated 90° along y-axis. Welin *et al.* 2010

TGART catalyzes the non-sequential steps 2, 3 and 5 of purine bisynthesis, which strongly suggests likely interactions between TGART and FGAMS, the enzyme that catalyzes step four. This implies that fl-HsTGART has disordered domains because it assumes an ordered conformation only when it is interacting with its binding partner. PPI between TGART and FGAMS is substantiated by fluorescent studies (16) and a modified Tango assay (15), which additionally showed PPAT interaction with TGART and FGAMS to nucleate the formation of

the purinosome [Fig. 8]. It is believed that this nucleate potentially acts as a scaffold for other purine synthesis protein. The PPAT and TGART interaction is suggested to be a means to transfer unstable substrate PRA from PPAT to TGART *via* substrate channeling. The kinetics model affirms that substrate diffusion is unlikely for substrates with half-life of 5 seconds such as PRA (13, 30). Co-purification of GART and AICART also implies PPI. These results provide evidence for interactions between these proteins however, the interacting interfaces, stoichiometry or the mechanism of the interaction is not yet known.

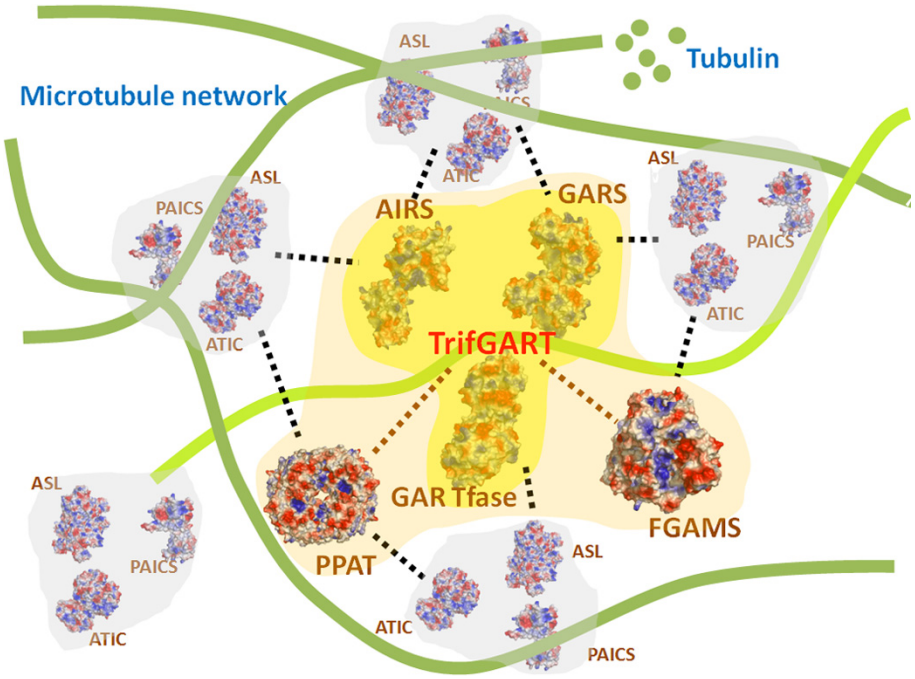

Figure 8 Interaction between the purinosome proteins: Tango assay confirmed presence of purinosome proteins interaction and gave an insight into purinosome core complex consisting of the first three enzymes of the *de novo* biosynthetic pathway, *Hs*PPAT, *Hs*TGART and *Hs*FGAMS. The nucleate also interacts with other purinosome proteins Deng *et al.* 2012

1.8 Implications of studying fl-*Hs*TGART

TGART is an integral protein in the *de novo* pathway for its enzymatic role and conceivably for forming a core complex of the purinosome. Fluorescent studies showed that increases in FGAMS and TGART co-clustering promoted purinosome complex formation and,

as reported by the Tango assay involves interactions between the *de novo* biosynthetic pathway enzymes. It is yet to be understood, however, whether this complex formation is a result of interaction between these proteins or is a means to increase the efficiency of the interaction. It is important to study the structure and higher order configuration of fl-*Hs*TGART to comprehend the molecular organization and interaction interfaces between these enzymes. A better understanding of the enzyme could also provide a framework for future drug discovery efforts.

2. Overall Goals

TGART is composed of GARS, GART and AIRS and catalyzes steps 2, 3 and 5 respectively in prokaryotes and eukaryotes. *E. coli* and related microorganisms have three mono-functional genes, whereas mammals express a trifunctional enzyme from a single gene for TGART. While X-ray crystal structure for individual domains for both *E. coli* and mammals have been solved, fl-*Hs*TGART structure is yet to be determined. Solution SAXS data (20) showed quaternary dimer configuration of fl-*Hs*TGART with extended disordered domains, which likely interacts with FGAMS to assume an ordered state. PPI assays demonstrated that PPAT, FGAMS and TGART potentially nucleate the purinosome complex. Despite identifying these characteristics of TGART, the findings are not adequate to fully realize its role in purinosome complex formation and *de novo* purine biosynthesis . Therefore, the goal of this works is to solve the crystal structure; to understand the molecular organization and nature of interactions with the other purine biosynthetic proteins and to characterize the kinetics of TGART in the complex. These studies will eventually help to understand if the purinosome complex is a result of the protein interactions or a way to increase interaction rate, and provide a more thorough understanding of the molecular determinants of purinosome structure.

2.1 Expression, purification and characterization of *Hs*TGART

In order to characterize the structure of the full-length TGART, fusion *Hs*TGART GARS-AIRS and AIRS-GART and a full length *Hs*TGART will be cloned, expressed and purified. These proteins will be used in crystallization trials in order to grow protein crystals for X-ray crystallography. In addition, the individual *Hs*TGART domains and fusion proteins, most of which have been purified, will be used in enzymes assays to monitor if existing in their different molecular configuration- individual, fusion or full length will affect their kinetics.

2.2 Quantitative and qualitative measurements of complex formation

The presence of purinosome (16) and protein-protein interactions (15) has been reported with help of qualitative means such as fluorescence imaging and a modified Tango assay, bothe conducted in cell culture. Absolute size exclusion chromatography (ASEC) and surface plasmon resonance (SPR) will enable examination of complex formation *in vitro* to give definitive, quantitative evidence for the interactions. Circular dichroism (CD) and small angle X-ray scattering under varying pH, salt and protein concentrations will be tested to elaborate the contingency of complex formation. These assays of complex configuration will be used both toexplore how complexation with the other proteins affects enzyme kinetics and also to identify conditions under which stable complexes form. A long term goal of this work is to conduct further investigation of stable complezes between TGART, FGAMS and PPAT using medium and high resolution approaches such as SAXS, cryo-electron microscopy and X-ray crystallography.

3. Progress

3.1 Cloning of individual and fused domains

Fl-*Hs*TGART cDNA was used as PCR template to generate individual domains (GARS, AIRS, GART) and fusion domain (AIRS-GART). Resultant PCR amplified sequences (GARS, AIRS, GART and AIRS-GART) were inserted into either pTHT (an in-house generated version of pET28a containing a TEV protease recognition site) or pET28a vector with kanamycin selection and N-terminal 6-His tag sequence. The insert plus vector ligations were sequenced for verification. The ligations were transformed into *E. coli* DH5α for plasmid amplification and Bl21 (DE3) for expression.

3.2 Protein expression

All four constructs were grown overnight in ten milliliters of LB with 100 ug/mL kanamycin at 37°C and the overnights were used to inoculate 1L LB (1:100 dilution). Cells were grown at 37°C until an optical density between 0.6 - 0.8 was reached and protein expression was induced with a final concentration of 100 uM IPTG (isopropyl β-D-1-thiogalactopyranosidase); protein was expressed overnight at 18°C. Cells were harvested by centrifugation (4200 *g*, 30 mins, 4°C).

3.3 Protein purification

Cells were resuspended in lysis buffer (300 mM sodium chloride, 50 mM sodium phosphate, 10mM imidazole, 10% glycerol, pH 7.66). For a pellet harvested from one liter, 10mL of lysis buffer was used and sonicated at 50% duty, power 7 for 5 minutes. The lysed cells were centrifuged (32,000 *g*, 45 mins. At 4°C). The supernatant was run through Ni-NTA column pre-equilibrated with lysis buffer at 4° C, (the individual constructs were manually purified using

benchtop while the fusion was purified using a Hi-Trap FF 1 mL Ni-NTA column on an AKTA Pure FPLC). The supernatant in the column was washed with 50 mL of wash buffer (300 mM sodium chloride, 50 mM sodium phosphate, 20 mM imidazole, 10% glycerol, pH 7.58) and eluted with 10 mL elution buffer (300 mM sodium chloride, 50 mM sodium phosphate, 250 mM imidazole, pH 7.55). The elution was buffer exchanged in a Sephadex pd10 column (Biorad) with 8 mL of storage buffer (25mM Tris-HCl, 1mM EDTA, 5 mM DTT, 10% glycerol, pH 7.40). Fusion AGT-GART underwent Cation exchange chromatography for further purification (MonoS 1mL column, GE). Post- purification, the constructs were analyzed using SDS-PAGE [Fig. 9].

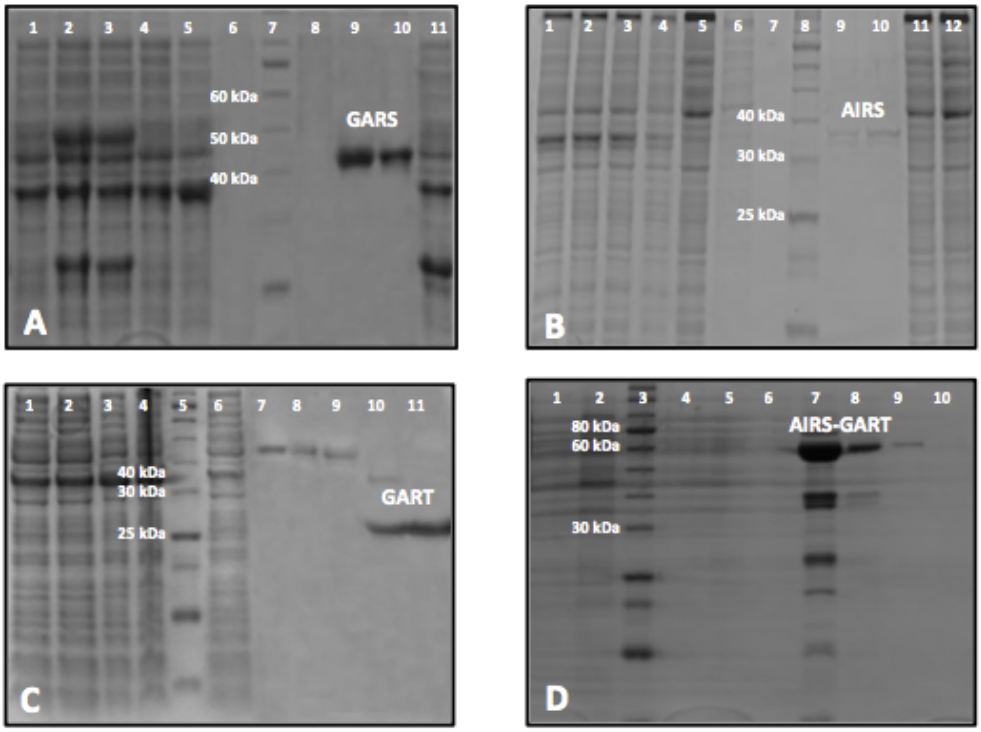

Figure 9 SDS-PAGE of purified *Hs*TGART:. All the proteins were 6-His tagged at the N-terminus. The soluble fraction was run through Ni-NTA affinity column at 4°C for purification. **A)** Lanes 9 and 10 show GARS bands of ~ 47 kDa. **B)** Lanes 10 and 11 show AIRS bands of~38kDa. **C)** Lanes 10 and 11 show GART bands of ~ 26kDa **D)** Lanes 7 and 8 show AGT-GART fusion protein bands of ~ 60kDa.

4. Future work

It has been established that fl-*Hs*TGART is a mono-functional gene product with three distinct domains GARS-ARIS-GART. Comparisons between individual TGART domains of *E. coli* and human have indicated high similarity. However, the fl-*Hs*TGART structure and its interacting surface with other proteins involved in *de novo* purine biosynthetic pathway have not been determined.

4.1 Expression and purification of TGART

To date the individuals domains (GART, AIRS and GART) [Fig. 8 A, B, C] and one fusion domain AIRS-GART [Fig. 8 D] of human TGART have been purified using Ni-NTA. While the individual domains had minimal co-purification with other proteins, AIRS-GART has been co-purified with proteins of sizes approximately 40kDa, 28 kDa and 23kDa. Cation exchange of the resultant Ni-NTA elution still yielded co-purification of AIRS-GART with these proteins. A possibility for separating 60kDa AIRS-GART from the smaller proteins is *via* gel filtration (size exclusion chromatography-SEC). Under non-reducing conditions AIRS-GART should dimerize so it will be expected to elute at an elution volume corresponding to a a size of approximately 120kDa in SEC. It is important to keep in mind that the oligomerization tendencies of 40kDa, 28kDa and 23kDa are unknown. If 40kDa form trimers, 28kDa and 23kDa form tetramers, they would elute with AIRS-GART dimers. If the size exclusion does not yield pure AIRS-GART, an alternative purification is immunoaffinity chromatography with GART domain epitope. An additional ion exchange step (either anion or cation exchange) could also be employed to further purify the protein.

Fl-*hs*TGART and fusion GARS-AIRS still need to be expressed and purified which will be done using same protocols followed for individual domains and AIRS-GART. Both the genes,

will be cloned in either pET 28a or pTHT which will provide N-terminal 6-His tag. The cloned genes will be sequenced and transformed into DH5α for plasmid growth and into BL21 (DE3) for protein expression. The cells will be lysed *via* sonication and the soluble fraction harvested *via* centrifugation will be run through AKTA (Ni-NTA) and will go under further purification steps (SEC, ion exchange) if required.

4.2 Determining structures of fl-*hs*TGART and TGART fusions

X-ray structures of individual human GARS, AIRS and GART have been determined but X-ray structures of neither the fusion (GARS-AIRS and AIRS-GART) nor the full-length have not been resolved. Purified human AIRS-GARS fusion and the fl-*Hs*TGART and fusion GARS-AIRS once purified in substantial amount (approximately 10mg/mL) will be used for crystal growth. Crystal growth conditions will be set up using manual hanging-drop vapor diffusion and robot sitting-drop vapor diffusion using sparse matrix screening. Crystal growth conditions will vary in pH, salt concentration, temperature; different protein concentrations will also be introduced, as well as various ligands to identify optimal conditions for protein crystal nucleation and growth.

Once crystallization conditions have been identified an doptimized the fusion proteins as well as the full-length protein will be crystallized with stable ligands. GARS will be crystallized with ATP and/or glycine. Ligands for GART are ATP, 10-formyl 5,8-dideazafolate, a stable analog of GART co-factor 10-formyltetrahydrofolate and GAR while AIRS ligands include FGAM and ATP. ATP, a common ligand in all three enzymes, could be replaced with its other analogs AMP-PNP or ATP-γS. If necessary to trap native ligands in the protein structures, we

will design and purify active site mutants of the proteins for additional structural analyses. Crystal data will be collected from synchrotron facilities at Cornell or Argonne national lab.

Fl-*Hs*TGART has disordered domains that could inhibit crystal formation and same difficulty might be encountered while crystallizing fusion proteins GARS-AIRS and AIRS-GART. It is worth looking into ways to stabilize the disordered regions to minimize conformational flexibility prior to setting up crystals. Circular dichroism (CD) of fl-*hs*TGART and fusion TGART with and without ligands can be measured and compared to determine if in presence of ligands the disordered domains form a less disordered structure. If necessary, these regions will be removed by mutagenesis in order to improve crystallizability. Alternatively, site-directed mutagenesis can be used to make single mutations that stabilize these regions.

4.3 Molecular organization and interactions measurements

Fellow lab members are tending to ongoing FGAMS and PPAT expression and purification. PPAT catalyzes step 1 which provides substrate PRA for GARS and FGAMS catalyzes step 5 producing FGAM, a substrate for AIRS.

4.3.1 Determining presence of interaction *via* quantitative means

4.3.1.1 Absolute size-exclusion chromatography (ASEC)

ASEC is combination of size exclusion chromatography (SEC) and dynamic light scattering (DLS). DLS measures the hydrodynamic radius of the molecules as they elute from SEC. SEC will help to estimate the approximate size of the individual protein and protein complex and determine the stability of the complex. Elution of protein complex is an indication that the complex is relatively stable. This will be fed to DLS, which will give an estimate on the

individual domain and protein complex radius of gyration. The latter will occur in presence of PPI and if present will also allow characterization of proximity of physical interaction. The differences in radius of gyration in polydisperse system, solutions containing more than one type of protein, for instance between fl-*hs*TGART-FGAMS, fl-*Hs*TGART-PPAT PPI, individual domains and FGAMS or PPAT and fusion TGART and FGAMS or PPAT, could be obtained and qualitatively measured using this method.

4.3.1.2 Surface plasmon resonance (SPR)

SPR is an optical technique to study label-free biomolecules interactions in real time. A single wavelength fixed angle light source hits the prism's base backside of a sensor chip and is reflected to the detector. The top of the stationary sensor surface will be fixed with either PPAT or FGAMS where untagged full-length or fusion TGART will be introduced. The reflected wavelength detected is different for association and dissociation of molecules. So in presence of interaction between the stationary protein (PPAT or FGAMS) and mobile analyte (TGART) the reflected wavelength over time gives the binding rate (κ_a) and protein dissociation over time gives unbinding rate (κ_d). This can be used to calculate the binding constant K_D ($K_D = \kappa_{d/} \kappa_a$).

4.3.2 Observing molecular organization using Small angle X-ray scattering (SAXS) and circular dichroism (CD) under varying conditions

An *et al.*'s SAXS data has indicated that fl-*Hs*TGART exists as a dimer in solution. Following the same path and upon isolation of a stable complex, SAXS will be used to determine the molecular organization of the individual and fusion TGART. This would show how the domains (individual- individual and fusion-fusion protein- protein interaction) interact with each other. SAXS data will also help in demonstrating higher order structure between fl-*hs*TGART

and other complexes, namely FGAMS and PPAT. Furthermore, CD will be used to observe changes in fl-*hs*TGART disordered domains when in complex with other proteins; this will help to explain the domains' function in organizing the higher order structure. These studies will be conducted both under physiological conditions and under varying pH, salt and protein concentration and in presence of ligands.

Conclusion:

TGART is a tri-functional enzyme that plays a critical role in purine biosynthesis and is believed to be structurally important for the purinosome. The goal of this work is to solve the crystal structure; to understand the molecular organization and nature of interactions with the other purine biosynthetic proteins and to characterize the kinetics of TGART in the complex.To this end, the three sub-domains of TGART and the fusion of AIRS-GART have been expressed and purified to homogeneity. Once the expression and purification of the remaining fusion and full length TGART have been completed, the structure and interactions of these proteins will be determined using X-ray crystallography, SAXS, ASEC and SPR. This work will provide needed details about the molecular determinants of purinosome structure and have the potential to identify new targets for future drug discovery efforts.

Work Cited

1. Smith GK, Mueller WT, Wasserman GF, Taylor WD, Benkovic SJ. Characterization of the enzyme complex involving the folate-requiring enzymes of de novo purine biosynthesis. Biochemistry-Us. 1980;19(18):4313-21.

2. Aimi J, Qiu H, Williams J, Zalkin H, Dixon JE. De novo purine nucleotide biosynthesis: cloning of human and avian cDNAs encoding the trifunctional glycinamide ribonucleotide synthetase-aminoimidazole ribonucleotide synthetase-glycinamide ribonucleotide transformylase by functional complementation in E. coli. Nucleic acids research. 1990;18(22):6665-72.

3. Jurecka A. Inborn errors of purine and pyrimidine metabolism. J Inherit Metab Dis. 2009;32(2):247-63.

4. Knox AJ, Graham C, Bleskan J, Brodsky G, Patterson D. Mutations in the Chinese hamster ovary cell GART gene of de novo purine synthesis. Gene. 2009;429(1-2):23-30.

5. Brodsky G, Barnes T, Bleskan J, Becker L, Cox M, Patterson D. The human GARS-AIRS-GART gene encodes two proteins which are differentially expressed during human brain development and temporally overexpressed in cerebellum of individuals with Down syndrome. Human molecular genetics. 1997;6(12):2043-50.

6. Dahms TE, Sainz G, Giroux EL, Caperelli CA, Smith JL. The apo and ternary complex structures of a chemotherapeutic target: human glycinamide ribonucleotide transformylase. Biochemistry-Us. 2005;44(29):9841-50.

7. Zhang Y, Morar M, Ealick SE. Structural biology of the purine biosynthetic pathway. Cellular and molecular life sciences : CMLS. 2008;65(23):3699-724.

8. Kappock TJ, Ealick SE, Stubbe J. Modular evolution of the purine biosynthetic pathway. Current opinion in chemical biology. 2000;4(5):567-72.

9. Poch MT, Qin W, Caperelli CA. The human trifunctional enzyme of de novo purine biosynthesis: heterologous expression, purification, and preliminary characterization. Protein expression and purification. 1998;12(1):17-24.

10. Li H, Fast W, Benkovic SJ. Structural and functional modularity of proteins in the de novo purine biosynthetic pathway. Protein science : a publication of the Protein Society. 2009;18(5):881-92.

11. Narayanaswamy R, Levy M, Tsechansky M, Stovall GM, O'Connell JD, Mirrielees J, et al. Widespread reorganization of metabolic enzymes into reversible assemblies upon nutrient starvation. P Natl Acad Sci USA. 2009;106(25):10147-52.
12. Havugimana PC, Hart GT, Nepusz T, Yang H, Turinsky AL, Li Z, et al. A census of human soluble protein complexes. Cell. 2012;150(5):1068-81.
13. Schendel FJ, Cheng YS, Otvos JD, Wehrli S, Stubbe J. Characterization and chemical properties of phosphoribosylamine, an unstable intermediate in the de novo purine biosynthetic pathway. Biochemistry-Us. 1988;27(7):2614-23.
14. Rudolph J, Stubbe J. Investigation of the mechanism of phosphoribosylamine transfer from glutamine phosphoribosylpyrophosphate amidotransferase to glycinamide ribonucleotide synthetase. Biochemistry-Us. 1995;34(7):2241-50.
15. Deng YJ, Gam J, French JB, Zhao H, An S, Benkovic SJ. Mapping Protein-Protein Proximity in the Purinosome. J Biol Chem. 2012;287(43):36201-7.
16. An S, Kumar R, Sheets ED, Benkovic SJ. Reversible compartmentalization of de novo purine biosynthetic complexes in living cells. Science. 2008;320(5872):103-6.
17. French JB, Zhao H, An SO, Niessen S, Deng YJ, Cravatt BF, et al. Hsp70/Hsp90 chaperone machinery is involved in the assembly of the purinosome. P Natl Acad Sci USA. 2013;110(7):2528-33.
18. An S, Deng Y, Tomsho JW, Kyoung M, Benkovic SJ. Microtubule-assisted mechanism for functional metabolic macromolecular complex formation. Proc Natl Acad Sci U S A. 2010;107(29):12872-6.
19. An S, Kyoung M, Allen JJ, Shokat KM, Benkovic SJ. Dynamic Regulation of a Metabolic Multi-enzyme Complex by Protein Kinase CK2. J Biol Chem. 2010;285(15):11093-9.
20. Welin M, Grossmann JG, Flodin S, Nyman T, Stenmark P, Tresaugues L, et al. Structural studies of tri-functional human GART. Nucleic acids research. 2010;38(20):7308-+.
21. Cheng YS, Shen Y, Rudolph J, Stern M, Stubbe J, Flannigan KA, et al. Glycinamide ribonucleotide synthetase from Escherichia coli: cloning, overproduction, sequencing, isolation, and characterization. Biochemistry-Us. 1990;29(1):218-27.

22. Galperin MY, Koonin EV. A diverse superfamily of enzymes with ATP-dependent carboxylate-amine/thiol ligase activity. Protein science : a publication of the Protein Society. 1997;6(12):2639-43.
23. Lee SG, Lutz S, Benkovic SJ. On the structural and functional modularity of glycinamide ribonucleotide formyltransferases. Protein science : a publication of the Protein Society. 2003;12(10):2206-14.
24. Manieri W, Moore ME, Soellner MB, Tsang P, Caperelli CA. Human glycinamide ribonucleotide transformylase: active site mutants as mechanistic probes. Biochemistry-Us. 2007;46(1):156-63.
25. Wang W, Kappock TJ, Stubbe J, Ealick SE. X-ray crystal structure of glycinamide ribonucleotide synthetase from Escherichia coli. Biochemistry-Us. 1998;37(45):15647-62.
26. Fawaz MV, Topper ME, Firestine SM. The ATP-grasp enzymes. Bioorg Chem. 2011;39(4-6):185-91.
27. Zhang Y, Desharnais J, Greasley SE, Beardsley GP, Boger DL, Wilson IA. Crystal structures of human GAR Tfase at low and high pH and with substrate beta-GAR. Biochemistry-Us. 2002;41(48):14206-15.
28. Li C, Kappock TJ, Stubbe J, Weaver TM, Ealick SE. X-ray crystal structure of aminoimidazole ribonucleotide synthetase (PurM), from the Escherichia coli purine biosynthetic pathway at 2.5 A resolution. Structure. 1999;7(9):1155-66.
29. Mueller EJ, Oh S, Kavalerchik E, Kappock TJ, Meyer E, Li C, et al. Investigation of the ATP binding site of Escherichia coli aminoimidazole ribonucleotide synthetase using affinity labeling and site-directed mutagenesis. Biochemistry-Us. 1999;38(31):9831-9.
30. Castellana M, Wilson MZ, Xu Y, Joshi P, Cristea IM, Rabinowitz JD, et al. Enzyme clustering accelerates processing of intermediates through metabolic channeling. Nature biotechnology. 2014;32(10):1011-8.